International Journal of Advanced Structural Engineering (2019) 11:385–394
https://doi.org/10.1007/s40091-019-00240-y

ORIGINAL RESEARCH

Evaluation and upgrading web-gap distortion retrofits in steel girder bridges

Mehdi Motaleb[1] · Ahmed Ibrahim[2] · Will Lindquist[3] · Riyadh Hindi[1]

Received: 28 January 2018 / Accepted: 20 August 2019 / Published online: 29 August 2019

Abstract

Distortion-induced fatigue cracking in the unstiffened web-gap of cross-frame diaphragms is the most prevalent type of cracking in steel girder bridges. Multi-steel girder bridges experience differential deflection between adjacent girders when subject to vertical loads resulting in a driving force in cross-frame diaphragms. The driving force developed in the cross-frame legs leads to out-of-plane distortion of the web-gap which results in high stress concentrations at the area, following by fatigue damages. This paper introduces an innovative method to retrofit web-gap distortion cracking, upgrade existing retrofits, and compare its effectiveness with two common retrofit techniques. The method involves cutting the existing connection plate and using angles to attach the disconnected part of the connection plate to the web. The method intends to eliminate the local high stresses at the connection plate end with considering minimal interference in original connection design and load path. Also, two other conventional repair methods were investigated, slot method and top-angle measure, to use as a basis for comparing the methods effectiveness. Laboratory testing was performed on a small-scale steel bridge bay by applying a vertical displacement to the free end of a cross-frame diaphragm to simulate the differential deflection between two adjacent girders in real bridges. The results from the testing were compared to findings from finite element analyses (FEA). Test results as well as FEA results for all investigated retrofit techniques are presented herein. Results showed that the newly developed slot-angle technique has significant potential for effectively reducing the stress concentrations in the web-gap region by removing the location of initial stress concentrations and redistributing those stresses over a wider area.

Keywords Steel bridge · Repair · Secondary cracking · Distortion-induced

Introduction

Connection between transverse diaphragms and longitudinal girders have been provided by connection plates (CPs) welded to the web and compression flange of many in-service bridges built in the United States prior to the mid-1980s (Jajich and Schultz 2003). Specifications prior to this time discouraged welding of these CPs to the tension flange as a standard design practice in order to avoid fatigue-sensitive transverse welds that previously resulted in fractures under primary loading (Khalil et al. 1998). Without a rigid connection between the CP and the flange, the torsional resistance of the bridge girder web is reduced. The imposed torsional force, moving from the diaphragm, enters the girder cross section at the CP and must be transmitted to the flanges. Therefore, the torsional deformation is concentrated in the unstiffened web-gap and results in out-of-plane bending of the web plate. The bending stress can easily exceed the

✉ Ahmed Ibrahim
aibrahim@uidaho.edu

Mehdi Motaleb
motalebm@slu.edu

Will Lindquist
lindquistw@william.jewell.edu

Riyadh Hindi
riyadh.hindi@slu.edu

[1] Parks College of Aviation, Engineering and Technology, Saint Louis University, St. Louis, MO 63103, USA

[2] Department of Civil and Environmental Engineering, College of Engineering, University of Idaho, Moscow, ID 83844, USA

[3] William Jewell College, Liberty, MO 64068, USA

specified yield stress of the steel for relatively high levels of distortion (Keating et al. 1997b).

Several experimental studies (Hartman 2013; Alemdar et al. 2013a), field-test measurements (Khalil et al. 1998; Shifferaw and Fanous 2013; Tarries 2002) and numerical analyses (Mahmoud and Miller 2015; Hartman et al. 2010; Alemdar et al. 2013b; Zhao and Kim Roddis 2007; Aygül et al. 2014) have been conducted to investigate distortion-induced fatigue cracking and to propose effective repair measures. However, selection of an appropriate repair strategy is complicated and depends on many factors (Alavi et al. 2017).

A previous study (Lindquist et al. 2015) evaluated distortion-induced fatigue cracks that developed in the web-gap region of a 1960's era design welded plate girder bridge shortly after completion of a comprehensive seismic retrofit. The main cause of cracking in that bridge was determined to be replacement of "K"-type diaphragms with much stiffer cross diaphragms resulting in stresses above the constant amplitude fatigue threshold (CAFT) (Motaleb et al. 2016). The results indicated that strengthening of existing bridge's structural elements could lead to unintended increases in stress (particularly in the web-gap area) and subsequent cracking. However, these high stress concentrations can be mitigated with additional retrofit measures prior to development of distortion-induced fatigue cracks leading to a reduction in future spending.

This paper examines the effectiveness of a newly developed web-gap retrofit methods compared with two existing popular retrofit techniques. The proposed method is also suitable for existing retrofits to prevent re-initiation of new cracks, as will be discussed in the following sections.

The laboratory test results of the retrofitted beams utilizing different retrofit techniques are compared. Testing was performed on a small-scale steel bridge bay by applying a vertical displacement to the free end of the cross-frame diaphragm to simulate the differential deflection between two adjacent girders in bridges. The results from the testing were compared to findings from finite element analyses (FEA). The details of the proposed technique with the findings are presented in the following sections.

Experimental program

The experimental testing was performed on a small portion of a steel bridge comprising a 1-m [3-ft] long standard hot rolled W24 × 55 girder, a concrete deck with dimension of 3.05 m × 2.13 m × 0.2 m (10 ft. × 7 ft. × 8 in.), and a cross-frame consisting of 2L2 × 2× ¼ angles connected to a CP through welded gusset plate, as shown in Fig. 1. The bottom flange of the girder was fixed to the deck using 12 A325 12.7 mm (5/8 in.) diameter post-installed bolts

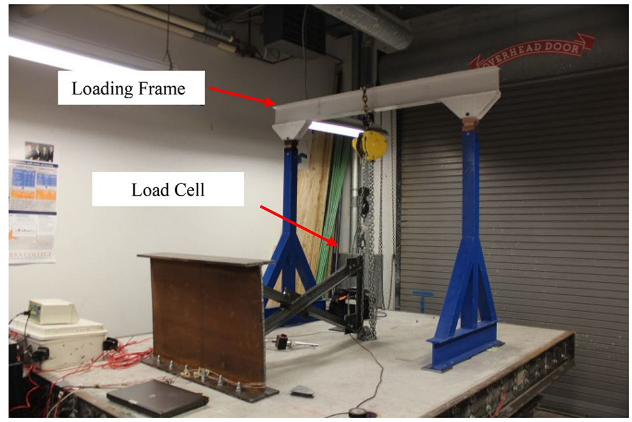

Fig. 1 Test setup

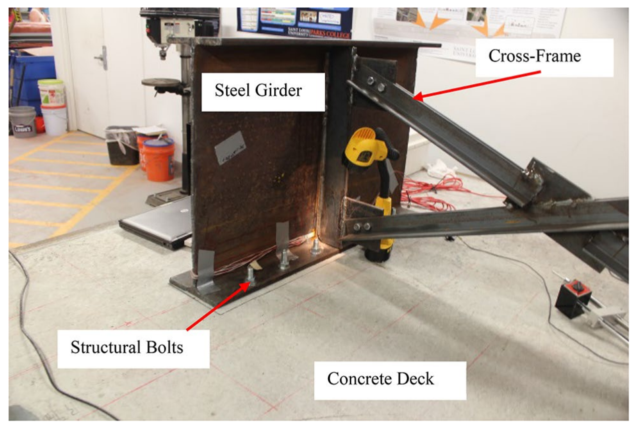

Fig. 2 Inverted steel–concrete beam

to simulate an inverse steel–concrete composite beam, as shown in Fig. 2. The structural steel properties are A992 for wide flange beam, and A36 for all angles and plates. The weld metal is E70xx and the welded members are connected by a minimum size of 6.35 mm (0.25 in.) fillet weld. A portable gantry crane was used as the loading tool for creating deflection by applying tension force through a load cell to the free end of the diaphragm. Before performing the test, the load cell location was checked to be located on the top of loading plate at the diaphragm ending to avoid inclined loading. The loading system was intended to approximately simulate the differential deflection between two girders in real bridges by applying upward vertical displacement. The system remained intact during the tests while the retrofit measures were implemented.

The authors used the same setup to conduct all the four retrofit cases and the reason for that is the beam was only loaded in the linear-elastic range, so no permanent deformations have been resulted from the loading protocol.

Strain gages layout

Three-element rosettes with compact geometry were used to determine the principal strains at the desired locations. These gages were positioned based on the predicted strain concentration locations before and after implementing the retrofit methods. The control beam was instrumented with three strain gages while strain gages 2 and 3 recorded the strains 12.7 mm (0.5 in.) and 19.1 mm (0.75 in.) left of the stiffener ending where it intersects the web. Strain gage "a" positioned on the opposite side of stiffener with distance of 5.08 mm (0.2 in.) from the stiffener. A schematic view of the strain gages layout is shown in Figs. 3 and 4.

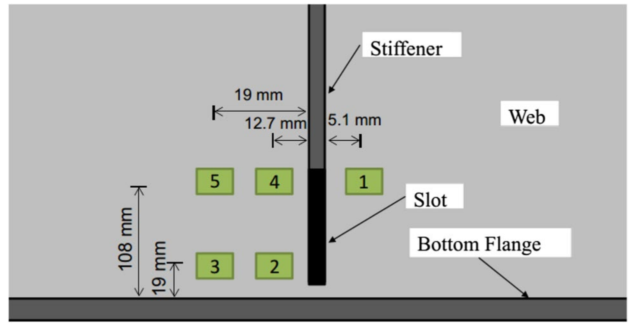

Fig. 4 Strain gage layouts for slot retrofit and slot-angle retrofit method

Retrofit measures

Several field and analytical investigations have been conducted to evaluate the effectiveness and feasibility of repairing members damaged by distortional stresses (Shifferaw and Fanous 2013; Fisher and Keating 1989; Zhao and Roddis 2000). In general, these retrofit options fall into one of two categories including (1) increasing the stiffness of the web-gap region by providing a positive attachment between the CP and the longitudinal girder flanges, or (2) increasing the flexibility of the web-gap region to reduce the concentration of stresses. Variations of both retrofit strategies are evaluated in conjunction with the innovative retrofit measures proposed herein.

The proposed retrofit technique consisted of a slot and an angle section connecting the disconnected part of the CP to the web. These retrofit measures intended to reduce stress levels by softening the web-gap region as well as distributing lateral forces, transferred by cross-frames, over a wider area of the web (slot-angle retrofit). This technique could be implemented to upgrade the existing slot repairs that failed to sufficiently fix distortion-induced fatigue cracking in the web-gap region. The Lexington Avenue Bridge in Lexington, KY, would be a good candidate for this repair strategy which experience re-initiation of fatigue cracks shortly after a softening retrofit was completed (Dexter and Ocel 2013).

Two other common retrofit methods (Dexter and Ocel 2013) are also considered in this study so that the effectiveness of the newly developed technique can be compared with popular repair methods. The first retrofit strategy provided a positive connection between the CP and the girder flange (referred to as the top-angle retrofit). The positive connection was provided using two angles located on both side of CP with snug tight bolted connection, as shown in Fig. 6. The second retrofit was made of a 89-mm (3.5-in.) slot where approximately one-sixth of the CP depth is cut from the web (slot-retrofit) softening of the web-gap. The slot was created by cutting the stiffener using an angle grinder. The cutting process was performed to simulate the actual field work by providing enough room for handling the grinder. Thus, there was a thin part of stiffener (about 0.25 in.) remained on the girder web. Figures 5, 6, 7 and 8 show the retrofit measures investigated in this paper. The main advantage of the slot-angle technique over top-angle option is that traffic interruption and lane closures are not necessary for implementation.

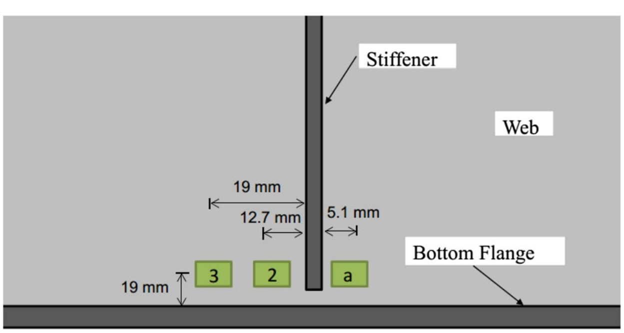

Fig. 3 Strain gage layouts for control beam and top-angle method

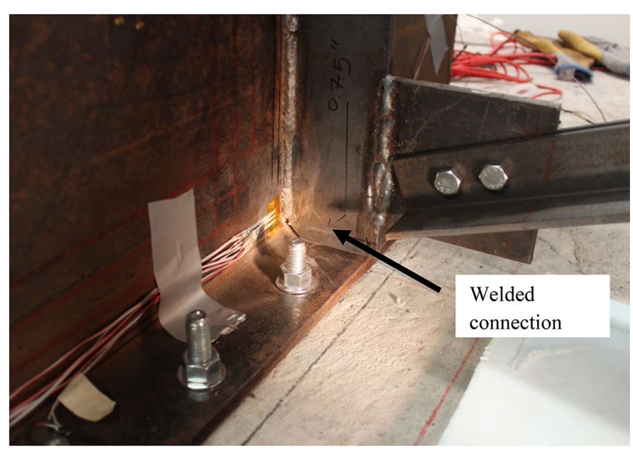

Fig. 5 Control beam

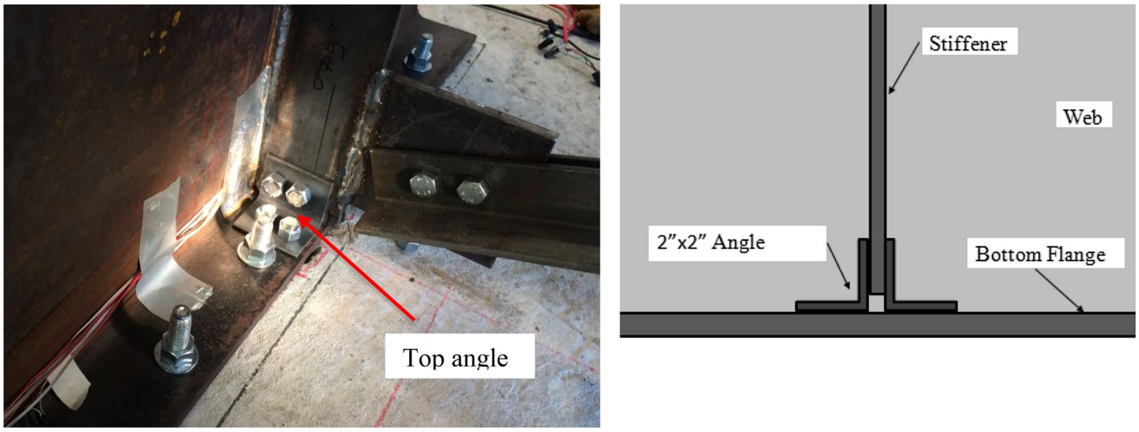

Fig. 6 Top-angle retrofit

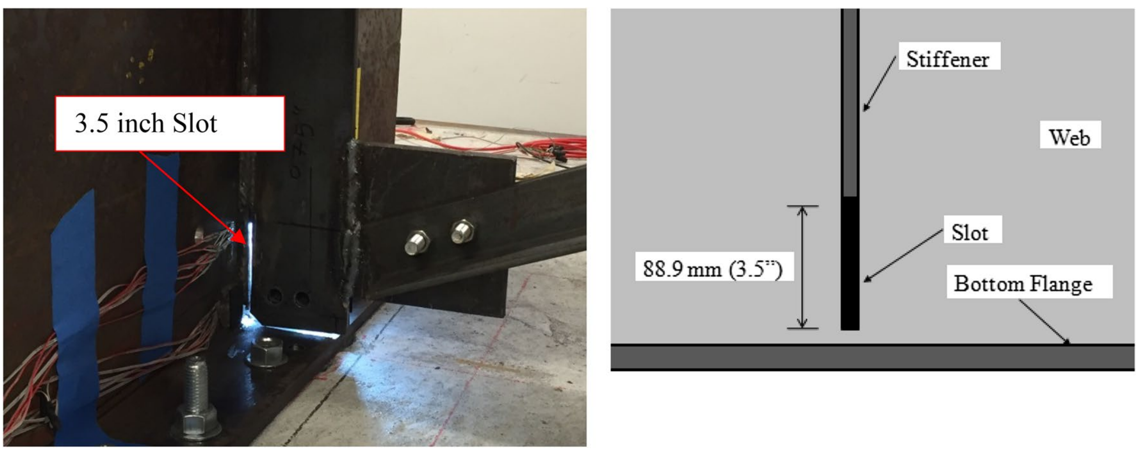

Fig. 7 Slot retrofit

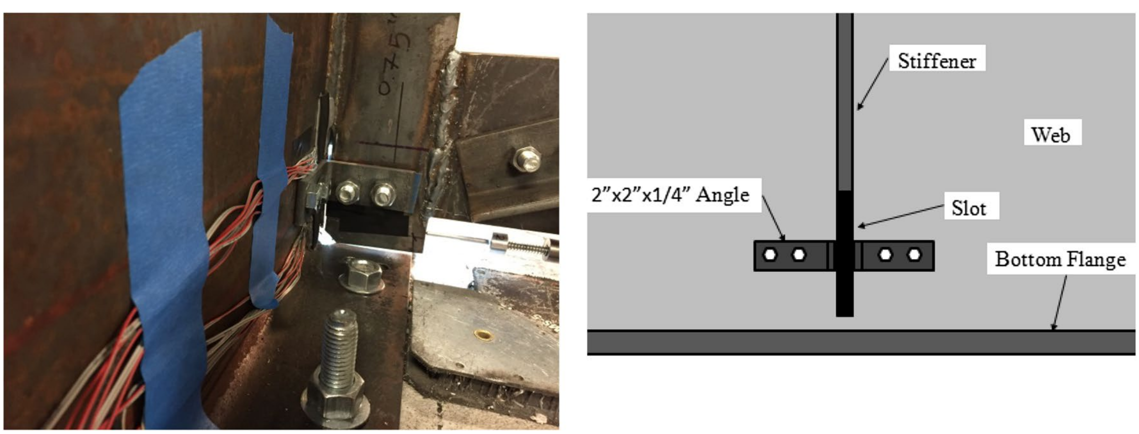

Fig. 8 Slot-angle retrofit

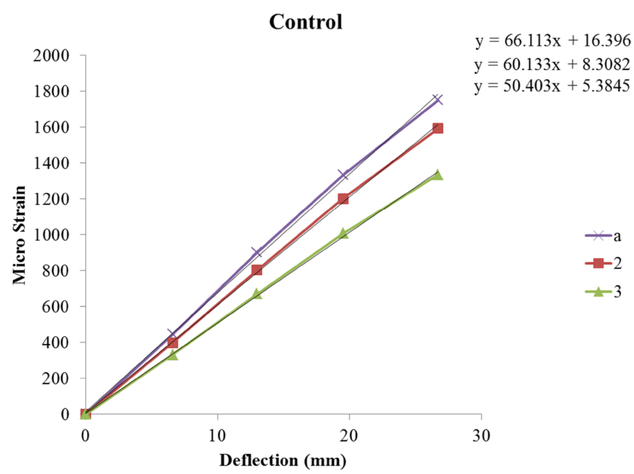

Fig. 9 Linear regression for 3 strain gages on control beam

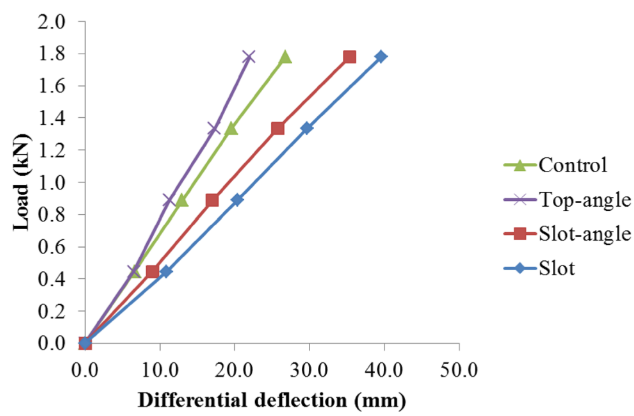

Fig. 10 Load versus differential deflection

Loading

Displacement control test was employed to create the differential deflection in the subcomponent tests rather than applying similar loads. This method provides deflection consistency between specimens with different retrofit options. The load of 1.78 kN (400 lbs.) was established as the maximum load for the control beam to prevent it from yielding, and was chosen as the maximum vertical load for all tests. The load was applied to the beams in four steps each with an interval of 445 N (100 lbs.) A load cell and LVDT were utilized to measure the applied load and deflections, respectively. The strain versus differential deflection was plotted for all cases. Linear regression was employed to find the equation through which the strain corresponding to any specific deflection can be determined. Figure 9 shows the linear regression for the three strain gages on the control beam.

The maximum load of 1.78 kN (400 lb.) on the retrofitted beam with the top-angle repair technique corresponded to a deflection of approximately 20.3 mm (0.8 in.). Since the top-angle specimen had the highest stiffness, as shown in Fig. 10, this displacement was used for all other three specimens. Figure 10 shows the applied vertical load versus vertical displacement of the diaphragm, and demonstrates that the top-angle method increased the stiffness of the whole beam connections while the slot and slot-angle methods increased the flexibility of the system.

Experimental results

The principal strains from 3-element gages were converted to stresses using Hook's law considering an elastic modulus of 200 GPa (29,000 ksi).

Each test was repeated three times to ensure consistency. Table 1 summarizes the results for each test. The stresses reported in this table correspond to the strain readings for the control and retrofitted beams under a 20.3 mm (0.8 in.) differential deflection. All stress values shown in Table 1 indicate various reductions in the elastic stress demand with respect to the control beam which varies between 14.8 and 62.0%. The slot technique reduced the stress in the original web-gap region by 62.0% and stress at the new CP–web intersection did not exceed 100 MPa (14.5 ksi)—far below the stress range in the control beam. The slot-angle retrofit method experienced 137 MPa (19.8 ksi)—a 44.4% reduction compared to the control beam. An L2 × 2× 1/8 angle was first used to connect the CP to the flange using two bolts on each leg (Fig. 6). The top-angle option showed the lowest reduction among the investigated options as it decreased the

Table 1 Laboratory test results

Web-gap stress (MPa) corresponding to 20.3 mm (0.8 in.) deflection							
Gage#	Control	Top-angle	Reduction (%)	Slot	Reduction (%)	Slot -angle	Reduction (%)
a	272	226	− 16.8				
1				88.3		43.5	
2	246	203	− 17.4	93.8	− 62.0	137	− 44.4
3	206	175	− 14.8	86.9	− 57.8	123	− 40.4
4				100		60.3	
5				95.1		61.1	

stresses from 14.8 to 16.8%. The stress distribution analysis for the retrofitted beams, as well as the control beam, will be discussed in the FEA section.

Top-angle results

To investigate the effect of the steel angle rigidity on the stress reduction in the web-gap region and susceptibility to distortion-induced fatigue damage, three different angle sections with a length of 50.8 mm (2 in.) were used to retrofit the beam. The three top-angle sections were L2 × 2× 1/8, L2 × 2× 1/4, and L2 × 2× 1/2. Figure 11 demonstrates the variation of the stresses in the web-gap region retrofitted with different angle sections and subjected to an equal displacement of 20.3 mm (0.8 in.) at the end of the diaphragm. There is only a small difference between stresses (ranging 3–8%) in the web-gap region of the retrofitted beams, as shown in Fig. 11.

Increasing the rigidity of the angle section limited the distortion in the web-gap region resulting in reducing the deflection of the cross-frame when subjected to a similar loading. However, when the beams are subjected to a similar deflection, there is only a minor change in stress, as shown in Fig. 11.

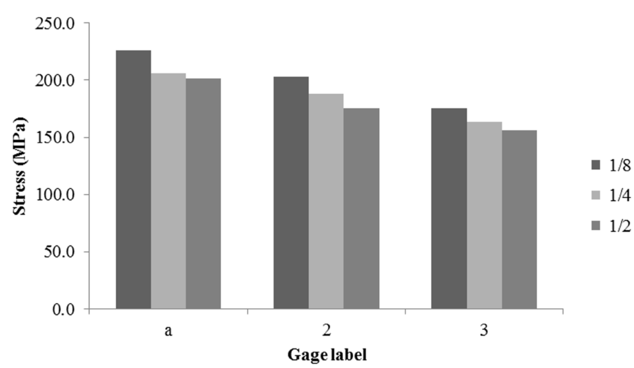

Fig. 11 Stresses for top-angle retrofitted beams due to 20.3 mm (0.8 in.) displacement

Finite element analysis

Four cases were considered for the FE analysis: a control beam, top-angle retrofitted beam (1/8-in. angle thickness), a slot-retrofitted beam, and a slot-angle retrofitted beam. Finite element models were developed to simulate the laboratory-tested beams and to establish a comparison of the stress distribution and distortion of the web-gap region. The FE models were created using 3D solid eight-node elements with three translational degrees of freedom and reduced integration (C3D8R) for all members including the girder, weld, gusset plate, CP, diaphragm, and loading plate. The girder was merged to the steel CP and the surrounding welding, and surface interactions with a penalty friction formulation was selected to define friction coefficients for bolted member's interfaces. Hard contact as normal behavior was used to minimize the penetration of adjacent surfaces in each other.

Loading was applied using a distributed load at the top of the loading plate at the end of the diaphragm on the opposite side of the girder. The girder was fixed to an 8-in. concrete deck. Figure 12 shows a perspective view of the model created using Abaqus/CAE (research license package).

Mesh density was determined by performing analyses with various element sizes in the web-gap region of the beam. The models contained approximately 50,000 elements, but varied slightly between the FE models based on the retrofit option evaluated. An element size of 2.54 mm (0.1 in.) was used in the web-gap region which converged to a constant value. A coarser mesh of 9.53 mm (0.375 in.) was used for the rest of the girder away from the location of interest. A mesh size of 25.4 mm (1 in.) was defined for the concrete.

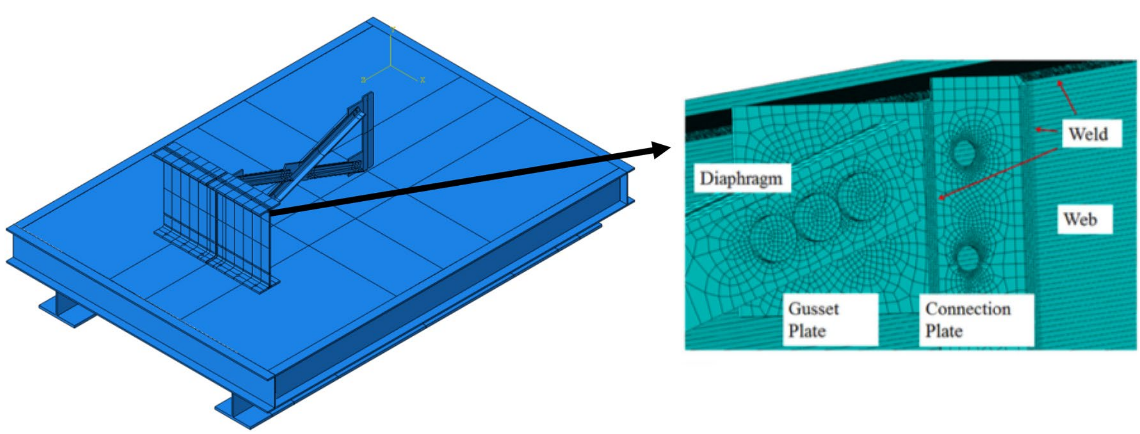

Fig. 12 3D view of the model created using Abaqus/CAE

Verification

The principal stresses at the locations corresponding to the attached strain gages in the lab test were determined and compared with the experimental results, as shown in Fig. 13. The results from the FEA are slightly higher than results from the lab test for the control beam and the retrofitted top-angle beam. For most of the readings from the gages attached to the retrofitted slot specimens, as well as slot-angle specimens, the corresponding stresses are moderately higher than those readings from the FEA. The percent difference between the experimental results and FEA results vary between 1 and 23%.

Stress distribution in the web-gap region

The stress distribution in the web-gap region varies based on the retrofit strategy. Figure 14a–d shows the principal stress contours when they are subjected to similar differential deflections. It should be noted that the retrofit angles in Fig. 14 are not shown for clarity. The spectrum is selected white and black with black color represents the highest stress not exceeding 345 MPa (50 ksi). The locations with stress greater than 345 MPa (50 ksi) are shown with grey. The control beam and top-angle retrofitted beam experience stress concentrations at the intersection of the web and the CP. However, the top-angle retrofit reduced the stress concentration values. The slot retrofit option managed to remove the stress concentrations from the CP ending while it introduces a new stress concentration location at the tip of the slot (Fig. 14c) where the CP is connected to the web. However, the new stress concentration area for the slot option is not as high as the control beam. The addition of the angle to reconnect the disconnected part of the CP to the web significantly reduced stress at the original stress concentration area as well as the new high stress zone introduced in the slot option (Fig. 14d). However, as it is shown in Figs. 8 and 14, there is a part of connection plate and welds remaining on the web after creating the slot. This remaining part provided unwanted stiffness to the web and created a higher stress zone compared to other areas.

Web-gap distortion

Keating et al. (1997a) determined high levels of distortion in the field and laboratory as 0.08 mm (0.003 in.) when measuring the relative displacement of the ends of the web-gap region. Although the recommended value for assessment of a retrofit option requires applying the actual differential deflection of the actual bridge under consideration and could be influenced by type and dimensions of girder and diaphragm, it still can comparatively provide an insight into the acceptable web-gap distortion for different retrofitted beams. Herein, the effectiveness of each retrofit option was examined by comparing the web-gap distortion caused by out-of-plane displacement in the web due to differential deflection of the cross-frame diaphragm. The web-gap distortion was determined for all

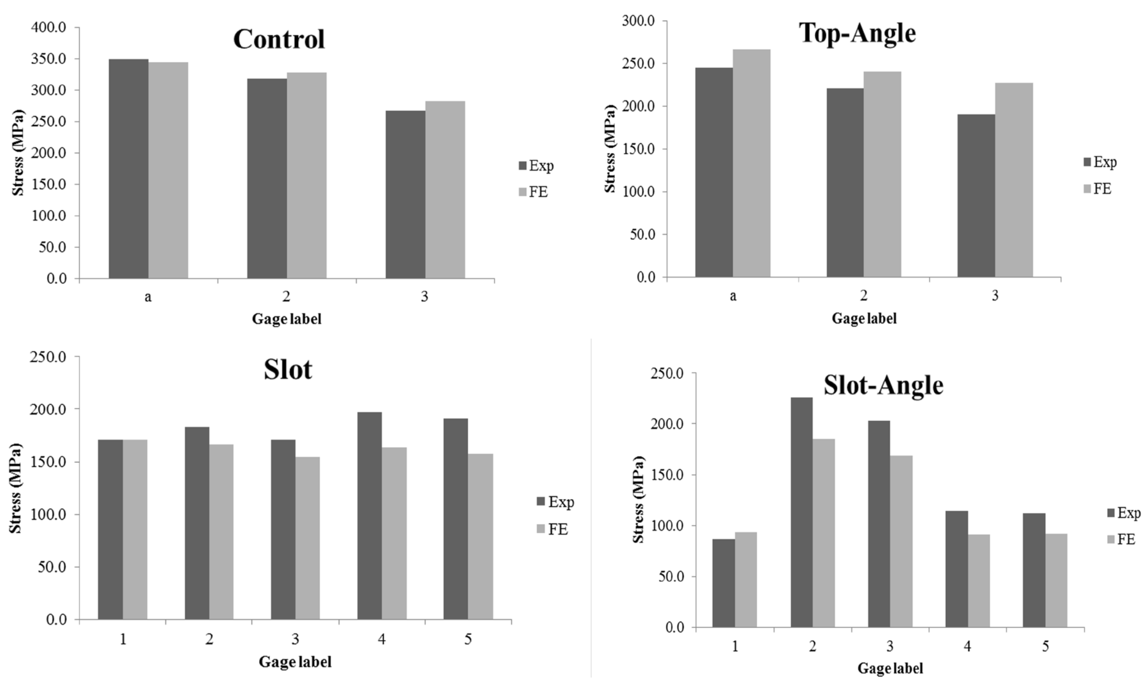

Fig. 13 Comparison between principal stresses from experimental test and FEA

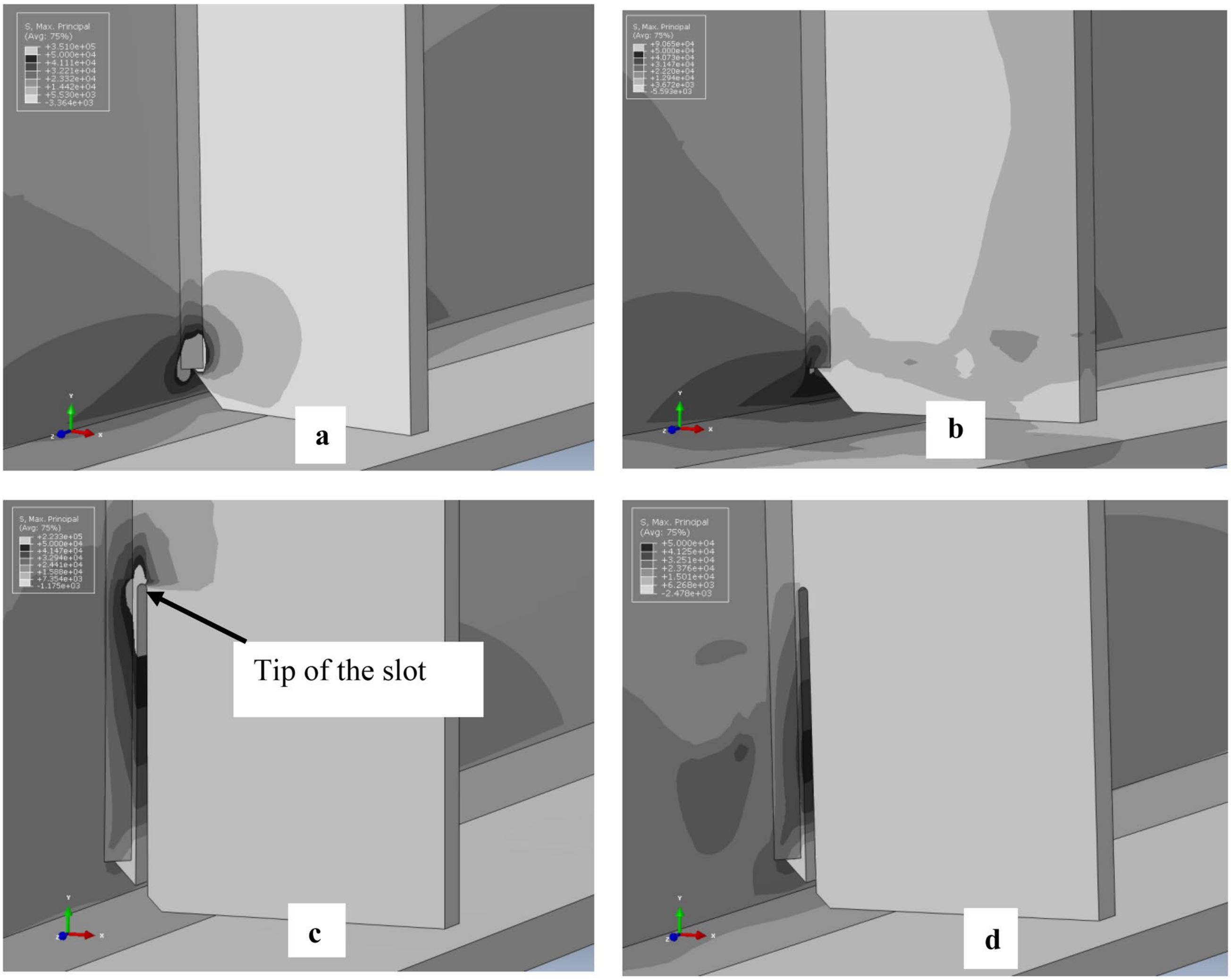

Fig. 14 Principal stress contours for **a** control beam, **b** top-angle retrofit, **c** slot retrofit, b slot-angle retrofit

four models along a 114-mm (4.5-in.) line on the web surface at the CP–web intersection. Since local displacement due to web-gap distortion is the primary concern in this study, the relative out-of-plane displacement is evaluated. The relative distortions are the out-of-plane displacement of the web excluding the global lateral displacement of the beam. Since the CP–web intersection was moved after creating the slot for the slot and slot-angle retrofit options, two sets of displacements are reported for these two retrofit options; first at the original intersection of the CP and web, and second, at the new intersection of the CP and web, as shown in Fig. 15.

Figure 16 demonstrates the relative distortion of the web in the web-gap region for all tested beams distortion in the web-gap region of beam when the cross-frame diaphragm is subjected to 20.3 mm (0.8 in.) deflection. The original line was used for measuring the distortion of control beam and top-angle specimens, while the distortion for slot repair

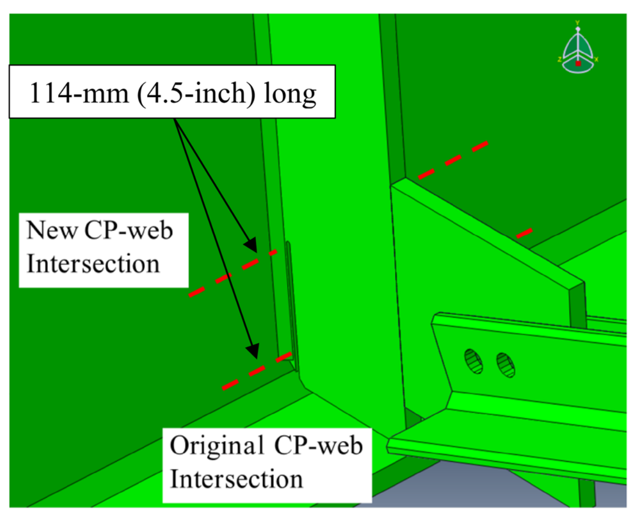

Fig. 15 Location of 114-mm (4.5-in.) lines for measuring relative distortion

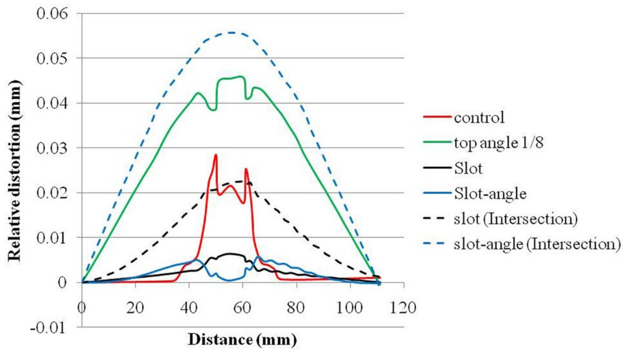

Fig. 16 Web-gap relative distortion along a 114-mm (4.5-in.) line

beam slot angle one was measure along the new line, shown in Fig. 16.

The control beam experienced a sudden increase in distortion at the CP–web intersection and exceeded 0.025 mm (0.001 in.). The retrofit options changed the distortion rate in the web-gap region. As shown in Fig. 16, where the localized distortion is more evenly distributed over a wider area when a retrofit measure is adopted. The top-angle method led to an increase in the web-gap out-of-plane displacement. However, the sudden increase for the control beam changed to a gradual increase in the web-gap distortion. Implementing slot and slot-angle retrofit options limited the distortion to a lower level. When the original lines at the CP–web intersection (solid lines), are considered as the reference for evaluating the results. The distortion for slot-angle exceeds 0.051 mm (0.002 in.) at the new CP–web intersection. However, the new web-gap region is more flexible than the original one to absorb the extra distortion.

Conclusions

In this paper, methods to retrofit the web-gap distortion and upgrade the existing retrofits were investigated. Also, the effectiveness of the proposed technique was compared with two other common retrofit techniques. This study was based on structural tests performed on a small portion of the bridge bay as well as conducting a FE analysis. The FE models were verified with experimental data and were used as a tool to evaluate the stress distribution in the web-gap region to determine fatigue-sensitive locations before and after implementing the retrofit options. This study has resulted in the following conclusions:

- The parametric study on the top-angle option showed that increasing the stiffness of the retrofitted elements slightly reduced the web-gap stress for specimens subjected to a differential deflection of 20.3 mm (0.8 in.).
- The slot retrofit option removed the stress concentrations from the CP end and introduced new stress concentrations at the slot termination point. While in terms of the magnitude and the high stress zone, they are not as large as the control beam. However, it has been shown that the concentrations are large enough to develop new cracking in some retrofitted bridges as discussed in Dexter and Ocel (2013).
- Based on the experimental and FE results, the slot-angle retrofit removed both the stress concentrations observed in the control and slot-retrofitted beams.
- Even though the experimental study showed that stresses significantly reduced in the web-gap after implementing the slot-angle method, the FE models showed that there was a higher stress zone in the remaining part of the CP on the web. It suggests the importance of minimizing the remained weld and plate after creating the slot.
- The slot-angle considerably reduced the web-gap stress and did not introduce a new fatigue-sensitive area in the girder based on the FE analysis, and showed a potential to be an effective method to restrain the out-of-plane displacement in steel bridge girders.
- The slot-angle method does not require disruption to the concrete deck and consequently to the traffic flow on the bridge. Also, this technique can be used to upgrade the slot retrofits implemented to the in-service bridges which started to reinitiate fatigue cracking in the web-gap regions after completion of the softening retrofit.

References

Alavi AH, Hasni H, Jiao P, Borchani W, Lajnef N (2017) Fatigue cracking detection in steel bridge girders through a self-powered sensing concept. J Constr Steel Res 128:19–38

Alemdar F, Nagati D, Matamoros A, Bennett C, Rolfe S (2013a) Repairing distortion-induced fatigue cracks in steel bridge girders using angles-with-plate retrofit technique. I: physical simulations. J Struct Eng 140(5):04014003

Alemdar F, Overman T, Matamoros A, Bennett C, Rolfe S (2013b) Repairing distortion-induced fatigue cracks in steel bridge girders using angles-with-plate retrofit technique. II: computer simulations. J Struct Eng 140(5):04014004

Aygül M, Al-Emrani M, Barsoum Z, Leander J (2014) Investigation of distortion-induced fatigue cracked welded details using 3D crack propagation analysis. Int J Fatigue 64:54–66

Dexter RJ, Ocel JM (2013) Manual for repair and retrofit of fatigue cracks in steel bridges. FHWA publication no. FHWA-IF-13-020

Fisher JW, Keating PB (1989) Distortion-induced fatigue cracking of bridge details with web gaps. J Constr Steel Res 12:215–228
Hartman A (2013) Analytical and experimental investigation for distortion-induced fatigue in steel bridges. Ph.D. dissertation. University of Kansas, project no. TPF-5(189)
Hartman AS, Hassel HL, Adams CA, Bennett CR, Matamoros AB, Rolfe ST (2010) Effects of cross-frame placement and skew on distortion-induced fatigue in steel bridges. Transp Res Rec 2200:62–68
Jajich D, Schultz AE (2003) Measurement and analysis of distortion-induced fatigue in multigirder steel bridges. J Bridge Eng 8:84–91
Keating P, Saindon K, Wilson S (1997a) Cross frame diaphragm fatigue and load distribution behavior in steel highway bridges. FHWA/TX-98/1360-2F, research report 1360-2F, TTI: 0-1360, final report
Keating PB, Saindon KC, Wilson SD (1997b) Cross frame diaphragm fatigue and load distribution behavior in steel highway bridges. FHWA/TX-98/1360-2F, research report 1360-2F, TTI: 0-1360, final report
Khalil A, Terry JW, Lowell G, Douglas LW, Bruce B (1998) Retrofit solution for out-of-plane distortion of X-type diaphragm bridges. In: Transportation conference proceedings, Iowa department of transportation, pp 99–102
Lindquist W, Ibrahim A, Tung Y, Motaleb M, Tobias D, Hindi R (2015) Distortion-induced fatigue cracking in a seismically retrofitted steel bridge. J Perform Constr Facil 30:04015068
Mahmoud HN, Miller PA (2015) Distortion-induced fatigue crack growth. J Bridge Eng 21:04015041
Motaleb M, Duong N, Lindquist W, Hindi R (2016) Investigation of distortion-induced web-gap cracking in a seismically retrofitted steel bridge: repair measures. J Bridge Eng 22:04016139
Shifferaw Y, Fanous FS (2013) Field testing and finite element analysis of steel bridge retrofits for distortion-induced fatigue. Eng Struct 49:385–395
Tarries DJ (2002) Diaphragm bolt loosening retrofit for web gap fatigue cracking in steel girder bridges. MS thesis. Lowa State University. https://doi.org/10.31274/rtd-180813-8049
Zhao Y, Kim Roddis WM (2007) Fatigue behavior and retrofit investigation of distortion-induced web gap cracking. J Bridge Eng 12:737–745
Zhao Y, Roddis WMK (2000) Fatigue crack investigation for the Arkansas river bridge in Hutchinson, Kansas. Constr Build Mater 14:287–295